Wall Carbonization in ASDEX: A Collation of Characteristic Results

W. Poschenrieder, G. Fußmann, G. v. Gierke, F. Mast, H. Niedermeyer, J. Roth, F. Söldner, K. Steinmetz, H. Verbeek, F. Wagner. G. Becker, H.S. Bosch, H. Brocken, K. Büchel, A. Eberhagen, D. Eckhartt, O. Gehre, J. Gernhardt, E. Glock, O. Gruber, G. Haas, J. Hofmann, A. Izvozchikov[1], G. Janeschitz, M. Kaufmann, F. Karger, M. Keilhacker[2], O. Klüber, M. Kornherr, K. Lackner, R.,S. Lang, M. Lenoci[3], F. Leuterer, G. Lisitano, H.M. Mayer, K. McCormick, D. Meisel, V. Mertens, H. Murmann, J.N. Noterdaeme, A. Pietrzyk[4], H. Rapp, H. Riedler, H. Röhr, F. Ryter[5], W. Sandmann, F. Schneider, C. Setzensack, G. Siller, P. Smeulders[2], E. Speth, K.-H. Steuer, O. Vollmer, F. Wesner, D. Zasche.

Max-Planck-Institut für Plasmaphysik, EURATOM-Association
D-8046 Garching/München, FRG

The aim of this presentation is to describe the procedures of carbonization and decarbonization followed on ASDEX, and to summarize the most significant changes of discharge parameters observed under the various experimental conditions with carbonized walls.

Carbonization and Decarbonization.

Carbonization, a method originally proposed by the Jülich IPP Group /1/ has been employed before on TEXTOR /2/ and JET /3/ to reduce high Z impurities from the wall material in discharges. In contrast to the philosophy on TEXTOR and JET, where carbonization was executed with wall temperatures above 150°C, room temperature conditions were used on ASDEX, without any obvious disadvantage. From August 85 to March 86 nine carbonization and five decarbonization runs were done. The walls were in carbonized condition on thirteen experiment days. The system for glow discharge cleaning /4/ was also employed here. Methane was admitted to the D_2 or H_2 discharge via the divertors to prevent local overconcentration. Typical discharge parameters during carbonization were $p(D_2) = 4.10^{-1}$ Pa and $p(CH_4) = 9.10^{-2}$ Pa with the discharge off. When the discharge is switched on (U = 400 V, I = 2.0 A) the partial pressures change as depicted in Fig. 1. The exponential transitions are reasonably well described by a first-order differential equation with the time constant given by $\tau^* = V/S$ for "off" and $\tau^* = V/(S_v + S^*)$ for "on". V is the vessel volume (26 m^3), S_v is the speed of the vacuum pumps, and S^* represents the speed by which CH_4 disappears from the gas phase caused by the discharge. H_2 shows practically the same time constants as CH_4 and is obviously produced by cracking of CH_4. The time constants yield S_v = 2600 l/s (only 1/4 of the full pumping system was employed) and S^* = 1500 l/s. The latter corresponds to a "cracking rate" of $3.5\ 10^{19}$ molec./s, while the current of 2A is equivalent to $1.2 \cdot 10^{19}$ ions/s. An analysis of the ions leaving the discharge by a time-of-flight analysis indicates that the current is mainly carried by hydrocarbon ions. Consistent with this is the observed deposition rate based on the table of interference colors as given by the Jülich group /5/. Obviously, CH_4 is more cracked than is directly deposited. The radicals

---

[1]Academy of Sciences, Lenigrad, USSR; [2]Assigned to JET Joint Undertaking, England; [3]ENEA Frascati, Italy; [4]University of Washington, Seattle, USA; [5]CEN Grenoble, France.

formed in the gas phase do not lead to carbonization on contact with the wall but seem to react to C_mH_n as indicated by the mass spectrum. A detailed particle balance was not attempted, but summing up the partial pressures of fig. 1 yields a slight increase of total pressure with the discharge on. It also explains the simultaneous drop in the ionization gauge indication since CH_4 is replaced by H_2 and HD.

The carbon deposition was limited to the plasma chamber, and not homogeneous owing to its geometry with corners and protrusions. Film thickness judged by the interference colors varied from 500 to 1500 Å, with a mean value of about 1000 Å after 6 hours carbonization. The deposited film were not analyzed otherwise, but all observations suggest they were the typical amorphous a-C:H layers /1/. Effect and behavior of the deposits during discharges are shown in fig. 2 for the radiation of C and Fe. Typically, one carbonization lasted for 50 shots (one experiment-day) with ICRH being most abrasive. The second carbonization was for 2h on top of the old layer.

Decarbonization in pure H_2 turned out to take about ten times as long as carbonization, i.e., 60 hours. But, the presence of a few permille of oxygen from residual H_2O, a leak or deliberate admission was found to considerably speed up the cleaning. A mixture of 0.5 % O_2 in H_2 reduced the time to 12 h, but lead to an increase of residual H_2O. A mixture of 5 to 10% O_2 in He cleaned the machine in less than 3 hours. It was followed by a deoxidation phase in a mixture of He and D_2 and pure D_2. (The best deoxidant is CH_4.) However, discharges after this procedure were characterized by poor density limits and other deviations from normality. Still, global radiation and O radiation were normal, but unusually high radiation of fluor (probably from decomposition of teflon) was found. So far, the actual origin of the problem remains unresolved.

The effects of carbonization on discharges

As already experienced previously with the large toroidal graphite limiter in ASDEX, the presence of large amounts of carbon in the plasma chamber can significantly affect the recycling behavior of hydrogen. Obviously, hydrogen atoms stick to the carbon surface without a high probability for recombination, as compared to steel at room temperature, thus large amounts of hydrogen stay in the vessel between shots. But, in contrast to JET, only minor problems with density control at very low densities were experienced. This is certainly due to the fact that the divertors, which dominate the recycling flux, remained uncarbonized.

ICRH: The success of carbonization reported from TEXTOR /2/, especially with respect to ion cyclotron resonance heating, was a strong motivation also to investigate carbonization on ASDEX. Indeed, concomitant with a reduction of central radiation from Fe by a factor of ten, the total ICRH power of 2.4 MW could now be launched. Without carbonization and only ohmic preheating the power limit was 1.1 MW due to disruptions caused by strong central Fe radiation. Typical values of P_{rad}/P_{tot} = 20 % were found and the improvement in radiation losses is also evident from Fig. 3 showing the fractional radiation increase per ICRH power coupled into the plasma for various wall conditions. Also, the degradation in τ_E during 1 MW of ICRH was only down to 70 % of the ohmic value, instead of 60 % for uncarbonized walls. A comparison of radiation profiles shows slightly increased boundary radiation for the carbonized case being mostly due to C radiation.

OH+NI: In the ohmic phase preceeding neutral injection, spectroscopic data show a 2.5-fold increase in C-radiation with carbonization, a slight decrease in O-radiation and a reduction of Fe-radiation by a factor of ten, still, the global radiation is little affected. Increased τ_E in the saturation regime ($n_e > 3\ 10^{19}\ m^{-3}$) as depicted in figure 4 indicates a reduced share of central radiation. This is fully corroborated by the radiation profiles showing the shift of major radiation to the boundary. Also for NI the degradation of energy confinement in the L-regime was less severe (figure 4), and the power limits for obtaining the H-regime in D_2-discharges were hardly influenced by carbonization. However, the H-regime was not of the same quality showing a higher and more stochastic ELM frequency. The difference is particularly obvious in the values of the poloidal beta, which reached only values of 55 % of the critical value instead of 70 % before carbonization. This behaviour might be associated with the increase in global radiation which is essentially due to high boundary radiation of C under carbonization.

LH: Also lower hybrid heating has profited from carbonization extending the working range to $5\ 10^{19}\ m^{-3}$. Radiation showed now a much smaller increase with $\bar{n}_e$ and LH-Power. Previously, the strong influence of Fe, caused by generated fast ions at higher density ($\bar{n}_e > 2\ 10^{19}\ m^{-3}$), had led to disruptions at $\bar{n}_e \approx 3.5 \times 10^{19}\ m^{-3}$. Problems with density control below $1.2\ 10^{19}\ m^{-3}$ limited the operation regime for experiments with current drive.

Pellet injection: Extremely high central densities of $2.2\ 10^{20}\ m^{-3}$ could now be reached as the reduced Fe-influx eliminated the thermal collapse observed without carbonization. The regime, thus attained, showed unusually long energy and particle confinement. The Murakami-parameter $\bar{n}\ R/B_T$ for $q = 2.7$ increased from $6\ 10^{19}\ m^{-2}\ T^{-1}$ (without carbonization) to $8.5\ 10^{19}\ m^{-2}\ T^{-1}$.

In conclusion, we see ICRH as the main beneficiary of carbonization but the reduced influx of heavy wall impurities extended the operational range quite generally. Only in the quality of the H-regime are negative effects of the increased boundary radiation seen. Carbonization can be regarded as a rather simple and efficient tool to change wall conditions and study plasma wall interaction. Though divertor discharges are less susceptible to impurities the results on ASDEX confirm those of TEXTOR and JET, all of which show that, for the time being, carbon is the best wall material.

References

/1/ Winter, Waelbroeck, Wienhold, Esser, Könen, Banno, Rota and Clausing, Journal of Nuclear Materials 122/123 (1984) 1187.
/2/ Schlüter, Graffmann, Könen, Waelbroeck, G. Waidmann, J. Winter and TEXTOR-Team, Proceed. 12th Europ. Conf. Controlled Fusion and Plasma Physics, Budapest (1985).
/3/ Bickerton et al. JET Report JET-P(85) 15.
/4/ Poschenrieder, Staudenmaier and Staib, Journal of Nuclear Materials 93/94 (1980) 322.
/5/ Winter, Wienhold, Besocke, Littmark, Esser, Banno, Waelbroeck, Kaleck and Tschersich, to be published.

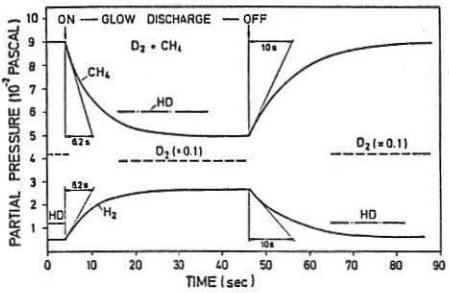

Fig.2: Variation of partial pressures of a D_2 + CH_4 mixture under stationary flow conditions, when the discharge is switched on.

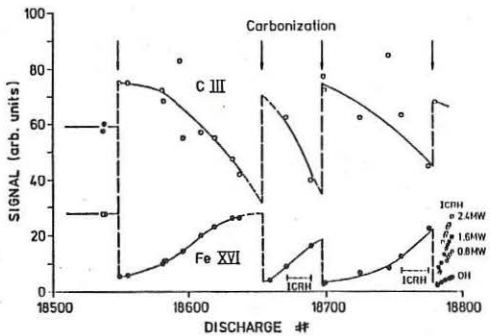

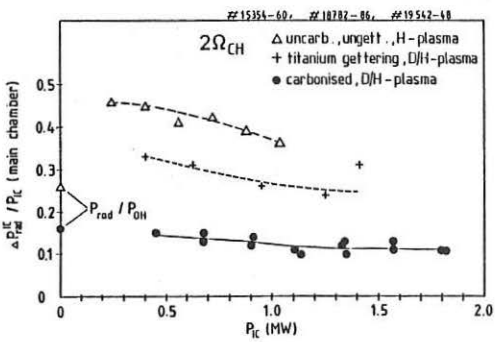

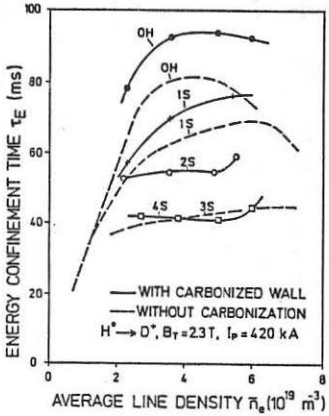

Fig. 4: Improvement of energy confinement with carbonization for OH- and NI-discharges (S: number of sources).

Fig.2: Effect of discharges on the carbon deposit, shown for Fe- and C-radiation. Points represent ohmic standard discharges where not indicated otherwise.

Fig. 3: Reduction of radiation increase during ICRH with carbonization.